



ELSEVIER

Journal of Chromatography A, 762 (1997) 35–46

JOURNAL OF  
CHROMATOGRAPHY A

# Molar enthalpy and molar volume of methylene and benzene homologues in reversed-phase liquid chromatography

Victoria L. McGuffin\*, Shu-Hui Chen<sup>1</sup>

*Department of Chemistry, Michigan State University, East Lansing, MI 48824, USA*

## Abstract

In this study, thermodynamic properties are measured for methylene and benzene homologues in reversed-phase liquid chromatography using octadecylsilica stationary phases and methanol mobile phase. The change in molar enthalpy ( $\Delta H^\circ$ ) is determined from graphs of the logarithm of the capacity factor versus the inverse temperature (15 to 60°C), whereas the change in molar volume ( $\Delta V^\circ$ ) is determined from graphs of the logarithm of the capacity factor versus pressure (830 to 5000 p.s.i.). For octadecylsilica phases with low bonding density ( $2.7 \mu\text{mol m}^{-2}$ ),  $\Delta H^\circ$  and  $\Delta V^\circ$  are small and are relatively unaffected by temperature and pressure. These thermodynamic parameters are linearly related to the homologue number for the methylene homologues, but not for the benzene homologues. For the ethylene group,  $\Delta\Delta H^\circ$  and  $\Delta\Delta V^\circ$  are in the order of  $-0.41 \text{ kcal mol}^{-1}$  and  $-1.0 \text{ cm}^3 \text{ mol}^{-1}$ , respectively, at 30°C. As the bonding density increases ( $5.4 \mu\text{mol m}^{-2}$ ), the molar volume and molar enthalpy decrease in a significant and nonlinear manner with the homologue number. Moreover, these thermodynamic parameters are markedly affected by temperature and pressure. For the ethylene group,  $\Delta\Delta H^\circ$  and  $\Delta\Delta V^\circ$  are in the order of  $-3.65 \text{ kcal mol}^{-1}$  and  $-14.1 \text{ cm}^3 \text{ mol}^{-1}$ , respectively, at 30°C. The theoretical and practical implications of these measurements are discussed with respect to the retention mechanism in reversed-phase liquid chromatography.

**Keywords:** Thermodynamic parameters; Retention mechanisms; Fatty acids; Polynuclear aromatic hydrocarbons

## 1. Introduction

Thermodynamic and other physicochemical measurements have been an essential and integral feature of chromatographic theory for many years [1,2]. They have enabled the estimation of activity coefficients, fugacities, virial coefficients, as well as other interaction parameters. In addition, they have been used to determine the equilibrium partition and/or adsorption coefficients, together with the concomitant changes in molar Gibbs free energy,

molar enthalpy, molar entropy, etc. Finally, they have been used to evaluate isotherms and to characterize phase transitions. Several recent reviews have summarized the present state of knowledge and state of the art in the application of thermodynamics to reversed-phase liquid chromatography [3–5].

Since chromatographic systems are dynamic in nature, one of the inherent challenges in making meaningful and accurate thermodynamic measurements is maintaining the appropriate constant conditions. Depending upon the thermodynamic parameters to be measured, the state variables of temperature, pressure, and/or volume may need to be carefully controlled. In most previous studies in reversed-phase liquid chromatography, including

\*Corresponding author.

<sup>1</sup> Present Address: Department of Chemistry, National Cheng Kung University, Tainan 70101, Taiwan.

those of Tchaplá et al. [3], Carr et al. [4], Wheeler et al. [5], Vailaya and Horváth [6], and many others, temperature has been well controlled but pressure has been allowed to fluctuate. In part, this oversight or neglect has been predicated on the widely held belief that compressibility of the mobile and stationary phases is not significant in liquid chromatography. However, several recent studies have demonstrated that this presumption may not be true under routine operating conditions [7,8].

To overcome this source of error, we have developed an experimental system that allows solute retention to be measured in situ at several positions along an optically transparent chromatographic column [9]. The resulting thermodynamic parameters are representative of a small isolated region of the column, wherein temperature and pressure are maintained relatively constant, rather than an average over the entire column length. In the present study, we have used this approach to determine the change in molar enthalpy and, for the first time, the change in molar volume for methylene and benzene homologues. As the elementary building blocks of organic molecules, the methylene and benzene groups are of fundamental significance. It is, therefore, desirable to characterize the thermodynamic behaviour of these groups in order to understand their effect upon retention in reversed-phase liquid chromatography.

## 2. Experimental methods

### 2.1. Reagents

The saturated, even-numbered fatty acid standards (Sigma, St. Louis, MO, USA) ranging from  $C_{10}$  to  $C_{22}$  are derivatized with 4-bromomethyl-7-methoxycoumarin as described previously [10]. The solvent is evaporated in a stream of dry nitrogen at  $40^{\circ}\text{C}$  and the residue is redissolved in methanol at a final concentration of  $10^{-4}$  M. The polynuclear aromatic hydrocarbon standards, consisting of phenanthrene, chrysene, picene, benzo[*a*]pyrene, tetrabenzonaphthalene, and phenanthro[3,4-*c*]phenanthrene (National Institute of Standards and Technology, Gaithersburg, MD, USA), are also prepared at  $10^{-4}$  M concentration in methanol. All organic solvents are high-purity, distilled-in-glass grade (Burdick &

Jackson Division, Baxter Healthcare, Muskegon, MI, USA).

### 2.2. Chromatographic system

The stationary phases are prepared by using an irregular silica material with particle size of  $5.5\ \mu\text{m}$ , pore size of  $190\ \text{Å}$ , and surface area of  $240\ \text{m}^2\ \text{g}^{-1}$  (IMPAQ 200, PQ Corp., Conshohocken, PA, USA). This material is reacted with monofunctional and trifunctional octadecylsilanes at bonding densities of  $2.7$  and  $5.4\ \mu\text{mol}\ \text{m}^{-2}$ , respectively, which correspond to surface coverages of  $0.34$  and  $0.68$  monolayer, respectively [11]. The microcolumns are fabricated from  $200\ \mu\text{m}$  I.D. fused-silica capillary tubing (Polymicro Technologies, Phoenix, AZ, USA), terminated with a quartz wool frit at a length of  $76.0$  cm. The polyimide coating is removed from the capillary at distances of  $23.2$ ,  $28.7$ ,  $52.8$  and  $58.3$  cm to facilitate on-column detection. A  $0.25\ \text{g}$  sample of the octadecylsilica material is suspended in  $1.0\ \text{cm}^3$  methanol. This slurry is introduced onto the capillary at  $5000\ \text{p.s.i.}$ , maintained at this pressure for  $2\ \text{h}$ , then gradually reduced to  $1000\ \text{p.s.i.}$  for  $10$  or more h ( $1\ \text{p.s.i.}=6894.76\ \text{Pa}$ ). The resulting microcolumns are evaluated under standard test conditions [12] to have a plate height of  $15\ \mu\text{m}$ , total porosity of  $0.84$ , and flow resistance parameter of  $500$ .

A schematic diagram of the experimental system is shown in Fig. 1. The methanol mobile phase is

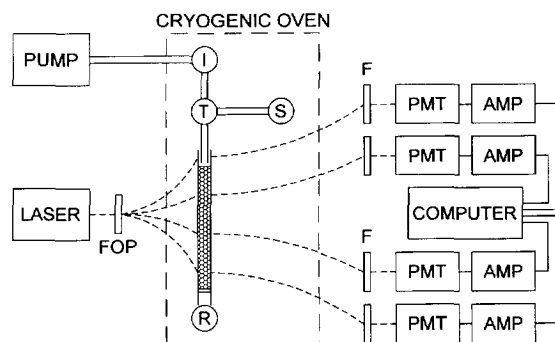


Fig. 1. Schematic diagram of experimental system for microcolumn liquid chromatography with on-column fluorescence detection. I = injection valve, T = splitting tee, S = splitting capillary, R = restricting capillary, FOP = fibre-optic positioner, F = filter, PMT = photomultiplier tube, AMP = current-to-voltage converter and amplifier.

delivered by a single-piston reciprocating pump (Model 114M, Beckman Instruments, San Ramon, CA, USA), operated in the constant-pressure mode ( $\pm 15$  p.s.i.). The sample is introduced by means of a 1.0 mm<sup>3</sup> injection valve (Model ECI4W1, Valco Instruments, Houston, TX, USA) and is subsequently split between the microcolumn and a 50  $\mu\text{m}$  I.D. fused-silica capillary (Polymicro Technologies), resulting in an injection volume of  $12 \times 10^{-3}$  mm<sup>3</sup>. A 20  $\mu\text{m}$  I.D. fused-silica capillary (Polymicro Technologies) is attached at the column outlet to serve as a restrictor. The column, injector, splitter, and restrictor are maintained at constant temperature ( $\pm 0.1^\circ\text{C}$ ) in a cryogenically cooled oven (Model 3300, Varian Associates, Sugar Land, TX, USA).

The experiments are conducted by systematically changing either pressure or temperature, while maintaining all other factors constant. For the pressure studies, the lengths of the restricting and splitting capillaries are proportionally decreased, so that the mobile phase linear velocity ( $0.08 \text{ cm s}^{-1}$  at room temperature) and split ratio (1:84) remain constant as the inlet pressure is reduced from 5000 to 830 p.s.i. As the temperature is decreased from 60 to  $15^\circ\text{C}$ , however, the linear velocity is allowed to change as a consequence of the variation in mobile phase viscosity with temperature. In this manner, the pressure drop along the column is maintained constant at 800 p.s.i. throughout the experiments. The local pressure at each detection position is then calculated by assuming a linear pressure drop ( $11 \text{ p.s.i. cm}^{-1}$ ) along the column. This calculation is verified by comparison with a more rigorous theoretical equation that accommodates the change in compressibility and viscosity of the mobile phase with both pressure [13] and temperature [14]. The deviation between the values calculated from the assumption of linear pressure and from the more rigorous nonlinear equation is found to be less than 1.4% for the experimental conditions of this study.

### 2.3. Detection system

A laser-induced fluorescence detection system, shown in Fig. 1, is utilized to examine the solute zones at four positions along the microcolumn. A continuous-wave He–Cd laser (Model 3074-20M, Omnichrome, Chino, CA, USA), with approximately

15 mW of power at 325 nm, is utilized as the excitation source. The laser radiation is transmitted to the microcolumn via small-diameter, UV-grade optical fibres (100  $\mu\text{m}$ , Polymicro Technologies), and fluorescence emission is collected in a right-angle geometry using optical fibres of larger diameter (500  $\mu\text{m}$ , Polymicro Technologies). The fluorescence emission at each detection position is isolated by an interference filter at 420 nm (Corion, Holliston, MA, USA) and is detected by a photomultiplier tube (Model R760, Hamamatsu, Middlesex, NJ, USA). The resulting photocurrent is amplified ( $100 \text{ nA V}^{-1}$ , 0.01 s time constant) and converted to the digital domain (Model 3405/5716, Data Translation, Marlborough, MA, USA). Data acquisition is performed by using the Forth-based programming language Asyst (Version 2.1, Keithley Asyst, Rochester, NY, USA) with an IBM-compatible computer. An acquisition rate of 1–5 Hz is employed to provide a minimum of 50 data points uniformly distributed across the solute zone profile.

### 2.4. Calculations

To characterize the solute zone profile, the method of statistical moments is chosen because it requires no assumptions concerning the mathematical form of the profile [15,16]. The statistical moments are calculated by finite summation of the fluorescence intensity as a function of time [ $F(t)$ ]:

$$M_0 = \sum F(t) dt \quad (1)$$

$$M_1 = \sum tF(t) dt / M_0 \quad (2)$$

The zeroth moment ( $M_0$ ) represents the area, while the first moment ( $M_1$ ) represents the centroid of the solute zone, which is the most accurate measure of the retention time.

The solute capacity factor ( $k$ ) in the region between any two detectors is calculated from the difference in the first moment between detectors ( $(\Delta M_1) = (M_1)_{\text{DET2}} - (M_1)_{\text{DET1}}$ ), evaluated for both the solute and the void marker:

$$k = \frac{(\Delta M_1)_{\text{SOLUTE}} - (\Delta M_1)_{\text{VOID}}}{(\Delta M_1)_{\text{VOID}}} \quad (3)$$

For this study, a fluorescent byproduct of the

coumarin derivatization reaction that coelutes with the injection solvent serves as a convenient and reliable void marker [7,17]. The accuracy of this void marker is verified from a graph of the logarithm of the capacity factor versus the solute carbon number. For the low-density monomeric stationary phase, the capacity factor for a solute with zero carbon number (*y* intercept) is  $0.047 \pm 0.001$  over all temperatures and pressures. For the high-density polymeric stationary phase, the capacity factor for a solute with zero carbon number is  $0.015 \pm 0.002$  in the temperature range from 20 to 40°C, and  $0.033 \pm 0.002$  in the temperature range from 50 to 60°C. Since these values are similar and approximately equal to zero, the use of this byproduct as a void marker can be approved.

It is noteworthy that the capacity factors determined by differential measurement between two on-column detectors are implicitly corrected for the effects of systematic (but not random) variations in temperature and pressure on the mobile-phase linear velocity as well as for extra-column effects [9]. With careful control of the temperature and pressure, the capacity factor for all model solutes is found to be constant along the column length. The precision of capacity factor measurements between the first and last detectors is better than  $\pm 0.4\%$  for capacity factors greater than 1.0, and  $\pm 1.5\%$  for capacity factors less than 0.30.

### 3. Results and discussion

From classical thermodynamics, the standard molar free energy ( $G^\circ$ ) is defined by the Gibbs-Helmholtz equation

$$G^\circ = H^\circ - TS^\circ \quad (4)$$

where  $H^\circ$  is the standard molar enthalpy,  $S^\circ$  is the standard molar entropy, and  $T$  is the absolute temperature. When applied to a solute that is in equilibrium between the mobile and stationary phases, the corresponding change in free energy is given by

$$\begin{aligned} \Delta G^\circ &= \Delta H^\circ - T\Delta S^\circ \\ &= -RT \ln K = -RT \ln(k\beta) \end{aligned} \quad (5)$$

where the solute capacity factor ( $k$ ) represents the thermodynamic equilibrium constant ( $K$ ) adjusted for the volumetric ratio of the mobile and stationary phases ( $\beta$ ). By rearrangement of this equation,

$$\ln k = \frac{-\Delta H^\circ}{RT} + \frac{\Delta S^\circ}{R} - \ln \beta \quad (6)$$

Thus, the change in molar enthalpy ( $\Delta H^\circ$ ) for the solute can be evaluated from a graph of the logarithm of the capacity factor versus the inverse temperature, provided that the phase ratio remains constant [1,2]. In this study, the experimental data are fitted by means of nonlinear regression using a combination of a linear equation, a second-degree polynomial equation, and a transposed second-degree polynomial equation, as necessary, to yield correlation coefficients ( $r^2$ ) greater than 0.99. The slope is then calculated by taking the partial derivative of the regression equation with respect to the inverse temperature. By using this approach, the molar enthalpy is determined with an average relative error of  $\pm 1.2\%$  for the low-density monomeric stationary phase and  $\pm 3.6\%$  for the high-density polymeric stationary phase over all temperatures and pressures.

The Gibbsian differential of the free energy is given by

$$dG^\circ = -S^\circ dT + V^\circ dP \quad (7)$$

where  $V^\circ$  is the standard molar volume and  $P$  is the pressure. When applied to a solute in equilibrium between the mobile and stationary phases, the corresponding differential equation is

$$\begin{aligned} d(\Delta G^\circ) &= -(\Delta S^\circ)dT + (\Delta V^\circ)dP \\ &= d[-RT \ln(k\beta)] \end{aligned} \quad (8)$$

and, by rearrangement,

$$\left( \frac{d(\ln k)}{dP} \right)_T = \frac{-\Delta V^\circ}{RT} + \left( \frac{d(\ln \beta)}{dP} \right)_T \quad (9)$$

Thus, the change in molar volume ( $\Delta V^\circ$ ) for the solute can be evaluated from a graph of the logarithm of the capacity factor versus the pressure at constant temperature, provided that the phase ratio remains constant [8,18]. In this study, the experimental data are fit by means of linear regression with correlation coefficients ( $r^2$ ) typically greater than 0.96. The slope is then calculated by the least-

squares method, which yields the molar volume with a constant average error of  $\pm 0.7 \text{ cm}^3 \text{ mol}^{-1}$  for the low-density monomeric stationary phase and  $\pm 1.3 \text{ cm}^3 \text{ mol}^{-1}$  for the high-density polymeric stationary phase. This results in a relative error that ranges from approximately  $\pm 10\%$  for a molar volume of  $10 \text{ cm}^3 \text{ mol}^{-1}$  to approximately  $\pm 1\%$  for a molar volume of  $100 \text{ cm}^3 \text{ mol}^{-1}$ .

Similarly, the Gibbsian differential of the enthalpy is given by

$$dH^\circ = TdS^\circ + V^\circ dP \quad (10)$$

The corresponding differential equation for a solute in equilibrium between the mobile and stationary phases is

$$d(\Delta H^\circ) = Td(\Delta S^\circ) + (\Delta V^\circ)dP \quad (11)$$

The partial derivative of this expression with respect to temperature is

$$\left(\frac{d(\Delta H^\circ)}{dT}\right)_P = T \left(\frac{d(\Delta S^\circ)}{dT}\right)_P = \Delta C_P \quad (12)$$

where  $\Delta C_P$  is the change in heat capacity at constant pressure.

### 3.1. Methylene homologues

To examine the behaviour of methylene homologues, a series of saturated even-numbered fatty acids ranging from  $C_{10}$  to  $C_{22}$  are chosen as model solutes. The change in molar enthalpy for these solutes is illustrated in Fig. 2. In all cases, the change in molar enthalpy is negative, which implies that the transfer of the solute from the methanol mobile phase to the octadecylsilica stationary phases is an exothermic process. For the low-density stationary phase (Fig. 2A), the molar enthalpy remains small and relatively constant throughout the examined temperature and pressure ranges. The values range from  $-1.74$  to  $-4.20 \text{ kcal mol}^{-1}$  for  $C_{10}$  to  $C_{22}$ , respectively, at  $30^\circ\text{C}$  and  $1330 \text{ p.s.i.}$  ( $1 \text{ cal} = 4.184 \text{ J}$ ). Moreover, the change in molar enthalpy per ethylene group ( $\Delta\Delta H^\circ$ ) calculated by difference between successive homologues remains relatively constant, as shown in Table 1, with an average value of  $-0.41 \pm 0.02 \text{ kcal mol}^{-1}$ . This suggests that each ethylene group contributes in an equal manner to the

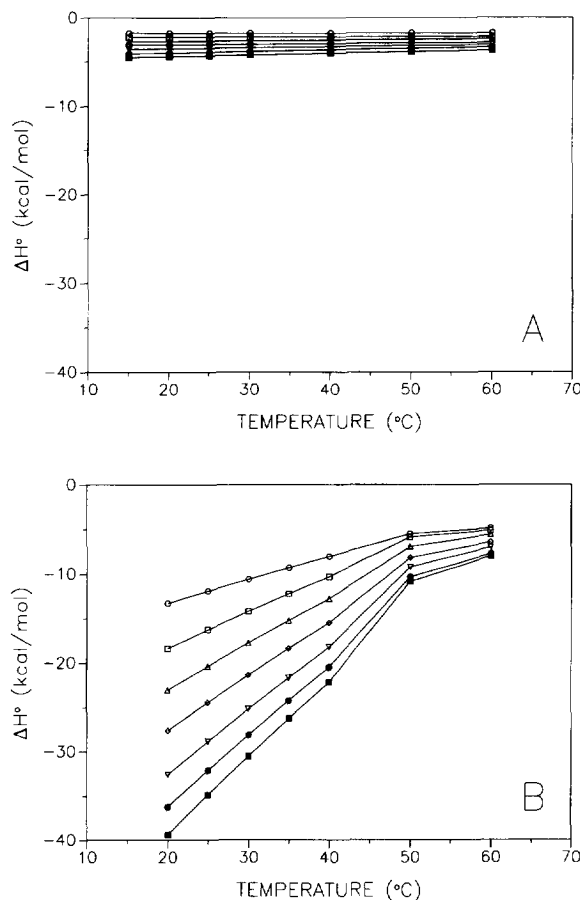


Fig. 2. Molar enthalpy ( $\Delta H^\circ$ ) as a function of temperature for the methylene homologues. (A) monomeric octadecylsilica stationary phase with  $2.7 \mu\text{mol m}^{-2}$  bonding density. (B) polymeric octadecylsilica stationary phase with  $5.4 \mu\text{mol m}^{-2}$  bonding density. Solutes: (○)  $C_{10}$ , (□)  $C_{12}$ , (Δ)  $C_{14}$ , (◇)  $C_{16}$ , (∇)  $C_{18}$ , (●)  $C_{20}$ , (■)  $C_{22}$ . Other experimental conditions as given in the text.

overall change in enthalpy for the homologous solutes.

For the high-density stationary phase (Fig. 2B), the change in molar enthalpy is significantly greater with values ranging from  $-10.6$  to  $-30.5 \text{ kcal mol}^{-1}$  for  $C_{10}$  to  $C_{22}$ , respectively, at  $30^\circ\text{C}$  and  $1470 \text{ p.s.i.}$  As shown in Table 1, the differential change in molar enthalpy per ethylene group remains constant for solutes  $C_{10}$  to  $C_{18}$ , within the statistical precision of the measurements. The average value of  $-3.65 \pm 0.13 \text{ kcal mol}^{-1}$  is approximately ten-fold higher than that for the low-density phase under the same conditions of temperature and pressure. How-

Table 1

Differential molar enthalpy ( $\Delta\Delta H^\circ$ ) and molar volume ( $\Delta\Delta V^\circ$ ) for the methylene homologues at 30°C

Solutes	Low-density octadecylsilica <sup>a</sup>		High-density octadecylsilica <sup>b</sup>	
	$\Delta\Delta H^\circ$ (kcal mol <sup>-1</sup> )	$\Delta\Delta V^\circ$ (cm <sup>3</sup> mol <sup>-1</sup> )	$\Delta\Delta H^\circ$ (kcal mol <sup>-1</sup> )	$\Delta\Delta V^\circ$ (cm <sup>3</sup> mol <sup>-1</sup> )
C <sub>12</sub> –C <sub>10</sub>	-0.45	-1.72	-3.63	-10.3
C <sub>14</sub> –C <sub>12</sub>	-0.39	-0.86	-3.54	-14.2
C <sub>16</sub> –C <sub>14</sub>	-0.40	-0.76	-3.60	-16.9
C <sub>18</sub> –C <sub>16</sub>	-0.40	-0.90	-3.84	-14.8
C <sub>20</sub> –C <sub>18</sub>	-0.42	-0.83	-2.91	-9.55
C <sub>22</sub> –C <sub>20</sub>	-0.41	-1.15	-2.39	-8.89

<sup>a</sup> Monomeric octadecylsilica stationary phase with 2.7  $\mu\text{mol m}^{-2}$  bonding density.<sup>b</sup> Polymeric octadecylsilica stationary phase with 5.4  $\mu\text{mol m}^{-2}$  bonding density.

ever, the solutes C<sub>20</sub> and C<sub>22</sub> have notably smaller enthalpy contributions of -2.91 and -2.39 kcal mol<sup>-1</sup>, respectively. These results are intuitively reasonable, based on the explanation proposed by Tchaplá et al. [3,19], as the additional carbon atoms in these solutes cannot be fully embedded in the octadecylsilica stationary phase.

It is also noteworthy that temperature and pressure exhibit a significant effect upon the molar enthalpy for the high-density stationary phase, in direct contrast to the low-density phase. As shown in Fig. 2B, the change in molar enthalpy for all solutes is linearly related to temperature in the range below 40°C. The slope, which represents the change in heat capacity at constant pressure ( $\Delta C_p$ ) according to Eq. (12), ranges from 0.26 to 0.86 kcal mol<sup>-1</sup> °C<sup>-1</sup> for C<sub>10</sub> to C<sub>22</sub>, respectively. There is a pronounced discontinuity between 40 and 50°C, which is consistent with previous reports of a phase transition for high-density octadecylsilica within this temperature region ([3,5,20] and references cited therein). It is also consistent with the behaviour of octadecanoic acid monolayers, which exhibit a half-expansion temperature of 46°C [21,22]. Above the transition temperature, the slope  $\Delta C_p$  is much smaller and ranges from 0.06 to 0.29 kcal mol<sup>-1</sup> °C<sup>-1</sup> for C<sub>10</sub> to C<sub>22</sub>, respectively.

The change in molar volume for the homologous solutes is illustrated in Fig. 3. In most cases, the change in molar volume is negative which implies that the solute occupies a smaller volume in the octadecylsilica stationary phases than in the methanol mobile phase. For the low-density stationary

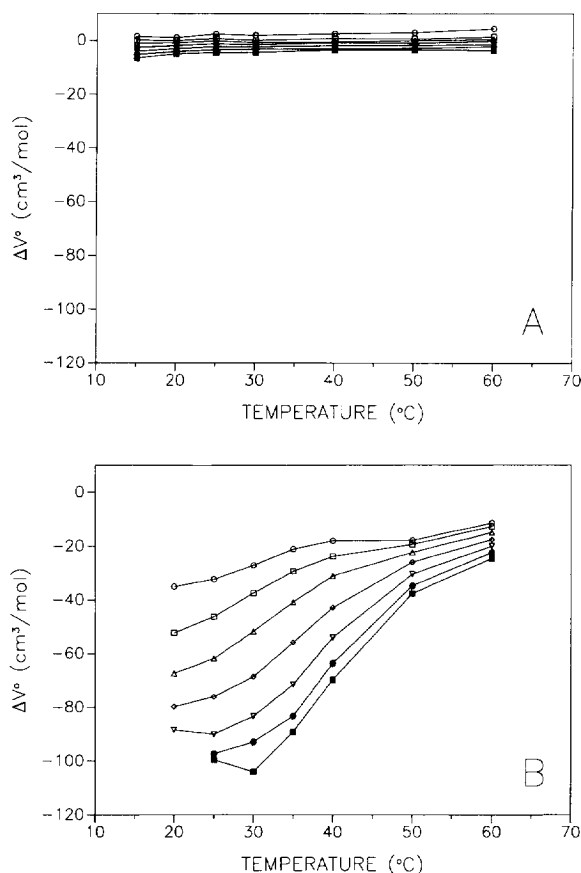


Fig. 3. Molar volume ( $\Delta V^\circ$ ) as a function of temperature for the methylene homologues. (A) monomeric octadecylsilica stationary phase with 2.7  $\mu\text{mol m}^{-2}$  bonding density, (B) polymeric octadecylsilica stationary phase with 5.4  $\mu\text{mol m}^{-2}$  bonding density. Solutes as given in Fig. 2; other experimental conditions as given in the text.

phase (Fig. 3A), the molar volume remains small and relatively constant throughout the examined temperature and pressure ranges. The values range from  $+1.92$  to  $-4.31 \text{ cm}^3 \text{ mol}^{-1}$  for  $C_{10}$  to  $C_{22}$ , respectively, at  $30^\circ\text{C}$ . The differential change in molar volume per ethylene group ( $\Delta\Delta V^\circ$ ) remains relatively constant, as shown in Table 1, with an average value of  $-1.0 \pm 0.4 \text{ cm}^3 \text{ mol}^{-1}$ . This suggests that each ethylene group contributes in an equal manner to the overall change in volume for the homologous solutes.

For the high-density stationary phase (Fig. 3B), the change in molar volume is significantly greater with values ranging from  $-27.1$  to  $-104 \text{ cm}^3 \text{ mol}^{-1}$  for  $C_{10}$  to  $C_{22}$ , respectively, at  $30^\circ\text{C}$ . As shown in Table 1, the differential change in molar volume per ethylene group remains constant for solutes  $C_{10}$  to  $C_{18}$ , within the statistical precision of the measurements. The average value of  $-14.1 \pm 2.8 \text{ cm}^3 \text{ mol}^{-1}$  is approximately ten-fold higher than that for the low-density phase under the same conditions of temperature and pressure. In order to gain an appreciation for the magnitude of this change, it is helpful to compare with the molar volume of the ethylene group in liquid octadecane. From the density of octadecane ( $0.7757 \text{ g cm}^{-3}$  at  $30^\circ\text{C}$  [23]), the molar volume of the ethylene group ( $28 \text{ g mol}^{-1}$ ) can be estimated as  $36 \text{ cm}^3 \text{ mol}^{-1}$ . Thus, the compression of the ethylene group in the high-density octadecylsilica stationary phase is approximately 39% of its total volume in the bulk liquid. The solutes  $C_{20}$  and  $C_{22}$  have notably smaller volume contributions of  $-9.55$  and  $-8.89 \text{ kcal mol}^{-1}$ , respectively, which represent compressions of the ethylene group by 27% and 25%, respectively, compared with the bulk liquid. Again, these results are intuitively reasonable because the additional carbon atoms cannot be fully embedded in the octadecylsilica stationary phase.

### 3.2. Benzene homologues

In order to examine the behaviour of benzene homologues, two series of model solutes have been selected. The first series consists of phenanthrene (Ph), chrysene (Chr), and picene (Pic), as shown in Fig. 4. These homologous polynuclear aromatic hydrocarbons have three, four, and five aromatic

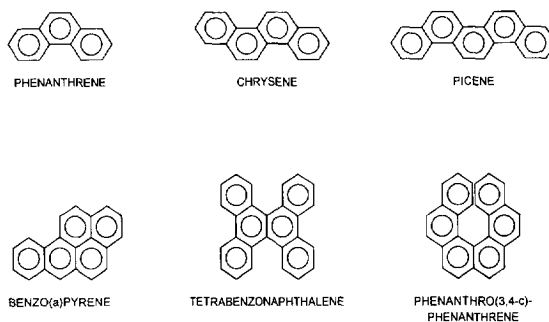


Fig. 4. Structure of benzene homologues used as model solutes.

rings, respectively, arranged in a planar cata-anneled structure [24]. The change in molar enthalpy for these solutes is illustrated in Fig. 5. In all cases, the change in molar enthalpy is negative which implies that the transfer of the solute from the methanol mobile phase to the octadecylsilica stationary phases is an exothermic process. For the low-density stationary phase (Fig. 5A), the molar enthalpy remains small and relatively constant throughout the examined temperature and pressure ranges. The values range from  $-0.83$  to  $-2.99 \text{ kcal mol}^{-1}$  for Ph to Pic, respectively, at  $30^\circ\text{C}$  and 1330 p.s.i. For the high-density stationary phase (Fig. 5B), the change in molar enthalpy is significantly larger with values ranging from  $-3.85$  to  $-17.2 \text{ kcal mol}^{-1}$  for Ph to Pic, respectively, at  $30^\circ\text{C}$  and 1470 p.s.i. The molar enthalpy remains relatively constant with temperature for Ph and Chr, but increases significantly for Pic with a slope  $\Delta C_p$  of  $0.19 \text{ kcal mol}^{-1} \text{ }^\circ\text{C}^{-1}$ . None of the homologous solutes exhibits a discontinuous change in molar enthalpy in the temperature region of the phase transition for octadecylsilica. Finally, we note that the differential change in molar enthalpy per benzene group ( $\Delta\Delta H^\circ$ ) is not constant for either the low-density or high-density stationary phase, as shown in Table 2. This suggests that each subsequent benzene group contributes more greatly to the overall change in enthalpy for the homologous solutes.

The change in molar volume for the homologous solutes is illustrated in Fig. 6. For the low-density stationary phase (Fig. 6A), the change in molar volume is positive which implies that the solute occupies a larger volume in the octadecylsilica stationary phases than in the methanol mobile phase.

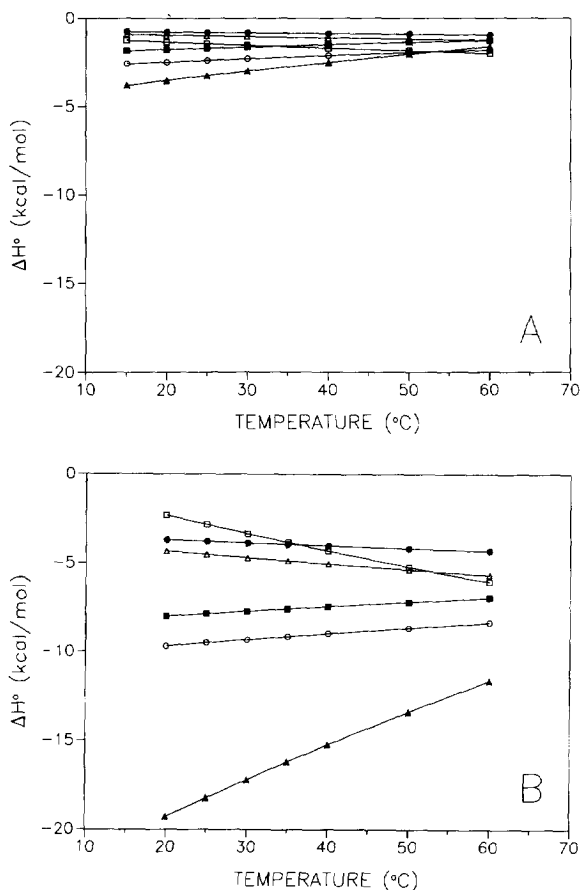


Fig. 5. Molar enthalpy ( $\Delta H^\circ$ ) as a function of temperature for the benzene homologues. (A) monomeric octadecylsilica stationary phase with  $2.7 \mu\text{mol m}^{-2}$  bonding density, (B) polymeric octadecylsilica stationary phase with  $5.4 \mu\text{mol m}^{-2}$  bonding density. Solutes: (●) phenanthrene, (■) chrysene, (▲) picene, (○) benzo[*a*]pyrene, (□) tetrabenzonaphthalene, (△) phenanthro[3,4-*c*]phenanthrene. Other experimental conditions as given in the text.

The values range from  $+6.27$  to  $+4.62 \text{ cm}^3 \text{ mol}^{-1}$  for Ph to Pic, respectively, at  $30^\circ\text{C}$ . For the high-density stationary phase (Fig. 6B), the change in molar volume is negative with values ranging from  $-2.01$  to  $-28.4 \text{ cm}^3 \text{ mol}^{-1}$  for Ph to Pic, respectively, at  $30^\circ\text{C}$ . The molar volume remains relatively constant with temperature for Ph and Chr, but increases significantly for Pic. Although there are minor perturbations, no clear discontinuity in molar volume is observed in the temperature region of the phase transition for octadecylsilica. Finally, the differential change in molar volume per benzene

group ( $\Delta\Delta V^\circ$ ) is not constant for either the low-density or high-density stationary phase, as shown in Table 2. This suggests that each subsequent benzene group contributes more greatly to the overall change in volume for the homologous solutes.

The second series of model solutes consists of benzo[*a*]pyrene (BaP), tetrabenzonaphthalene (TBN), and phenanthro[3,4-*c*]phenanthrene (PhPh), also shown in Fig. 4. This combination of planar and nonplanar polynuclear aromatic hydrocarbons has been used to evaluate the selectivity of octadecylsilica stationary phases by Sander and Wise [20,25]. For the low-density stationary phase, the elution order is  $\text{PhPh} < \text{BaP} < \text{TBN}$  throughout the examined temperature and pressure ranges. The selectivity factors ( $\alpha$ ) for the nonplanar solutes TBN and PhPh relative to the planar solute BaP are 1.66 and 0.75, respectively, at  $30^\circ\text{C}$ . Thus, this stationary phase is consistent with intermediate or oligomeric behaviour in the classification scheme developed by Sander and Wise [20,25]. For the high-density stationary phase, the elution order is  $\text{PhPh} < \text{TBN} < \text{BaP}$  throughout the examined temperature and pressure ranges. The selectivity factors for TBN and PhPh relative to BaP are 0.43 and 0.24, respectively, at  $30^\circ\text{C}$ . Thus, this stationary phase is consistent with polymeric behaviour in the classification scheme of Sander and Wise [20,25].

The changes in molar enthalpy and molar volume for these solutes are shown in Figs. 5 and 6, respectively, and the differential changes are summarized in Table 2. Several salient conclusions may be drawn from these results. First, the general trends of behaviour for the planar solute BaP are similar to those of the other planar benzene homologues discussed previously. BaP has a peri-condensed structure with correspondingly smaller length-to-breadth ratio [20,26] and larger minimum area [27] than Pic, the cata-annelated homologue with the same number of aromatic rings. Thus, the changes in molar enthalpy and volume for BaP are smaller in magnitude than those for Pic. In contrast, the nonplanar solutes TBN and PhPh show distinctly different trends. The changes in molar enthalpy and volume for these six-ring nonplanar solutes are most comparable to the three-ring planar solute Ph, which serves as a building block in their structures. The change in molar enthalpy for TBN and PhPh decreases with



Table 2  
Differential molar enthalpy ( $\Delta\Delta H^\circ$ ) and molar volume ( $\Delta\Delta V^\circ$ ) for the benzene homologues at 30°C

Solutes	Low-density octadecylsilica <sup>a</sup>		High-density octadecylsilica <sup>b</sup>	
	$\Delta\Delta H^\circ$ (kcal mol <sup>-1</sup> )	$\Delta\Delta V^\circ$ (cm <sup>3</sup> mol <sup>-1</sup> )	$\Delta\Delta H^\circ$ (kcal mol <sup>-1</sup> )	$\Delta\Delta V^\circ$ (cm <sup>3</sup> mol <sup>-1</sup> )
Chr–Ph	–0.80	–0.58	–3.86	–6.56
Pic–Chr	–1.36	–1.07	–9.48	–19.9
Pic–BaP	–0.70	–0.54	–7.87	–18.1
PhPh–Ph	–0.20	+3.23	–0.84	+3.22
TBN–BaP	+0.76	+3.55	+5.99	+17.1
PhPh–BaP	+1.26	+4.35	+4.63	+11.6
PhPh–TBN	+0.49	+0.80	–1.36	–5.50

<sup>a</sup> Monomeric octadecylsilica stationary phase with 2.7  $\mu\text{mol m}^{-2}$  bonding density.

<sup>b</sup> Polymeric octadecylsilica stationary phase with 5.4  $\mu\text{mol m}^{-2}$  bonding density.

increasing temperature for both low-density and high-density stationary phases. This gives rise to a negative change in the heat capacity at constant pressure ( $\Delta C_p$ ) of  $-0.09$  and  $-0.03$  kcal mol<sup>-1</sup> °C<sup>-1</sup> for TBN and PhPh, respectively. The change in molar volume is positive for both stationary phases, however it increases slightly with temperature for the low-density stationary phase and decreases significantly with temperature for the high-density stationary phase. Finally, we note in Table 2 that the low-density stationary phase is characterized by an increase in  $\Delta\Delta H^\circ$  and  $\Delta\Delta V^\circ$  for TBN with respect to BaP, for PhPh with respect to BaP, and for PhPh with respect to TBN. The high-density stationary phase is characterized by an increase in  $\Delta\Delta H^\circ$  and  $\Delta\Delta V^\circ$  for TBN with respect to BaP and for PhPh with respect to BaP, but a decrease in  $\Delta\Delta H^\circ$  and  $\Delta\Delta V^\circ$  for PhPh with respect to TBN. Thus, the changes in selectivity between oligomeric and polymeric behaviour identified by Sander and Wise [20,25] appear to be derived from the differential changes in molar enthalpy and volume for the nonplanar solutes PhPh and TBN.

### 3.3. Comparison of methylene and benzene homologues

Based on the results presented above, there are several similarities and distinctions that characterize the thermodynamic behaviour of methylene and benzene homologues in reversed-phase liquid chro-

matography. First, it is instructive to compare the behaviour of homologues with the same carbon number (e.g., C<sub>14</sub> and Ph, C<sub>18</sub> and Chr, C<sub>22</sub> and Pic) in Tables 3 and 4. The methylene homologues exhibit a significantly greater change in molar enthalpy than do the corresponding benzene homologues for both the low-density and high-density stationary phases. This distinction arises because the physical and chemical structure of the methylene homologues is identical to the octadecylsilica stationary phase. This template structure allows the most favourable alignment of each methylene group and, hence, the greatest total enthalpy of interaction. For similar reasons, the change in molar volume is also significantly greater for the methylene homologues than for the corresponding benzene homologues. The template structure allows the methylene groups to fit and conform most closely to the interstices between octadecyl chains in the stationary phase.

The changes in molar enthalpy and volume are linearly related to the homologue number for the methylene homologues, which suggests that each group contributes equivalently to retention. It is, therefore, not surprising that the molar enthalpy and volume show a linear correlation, as summarized in Table 3. Although the benzene homologues do not exhibit the same linear relationships with homologue number, a linear correlation is nevertheless observed between the molar enthalpy and volume, as summarized in Table 4. The thermodynamic basis of this enthalpy–volume correlation will be discussed in future work [28]. It is noteworthy that the slope,

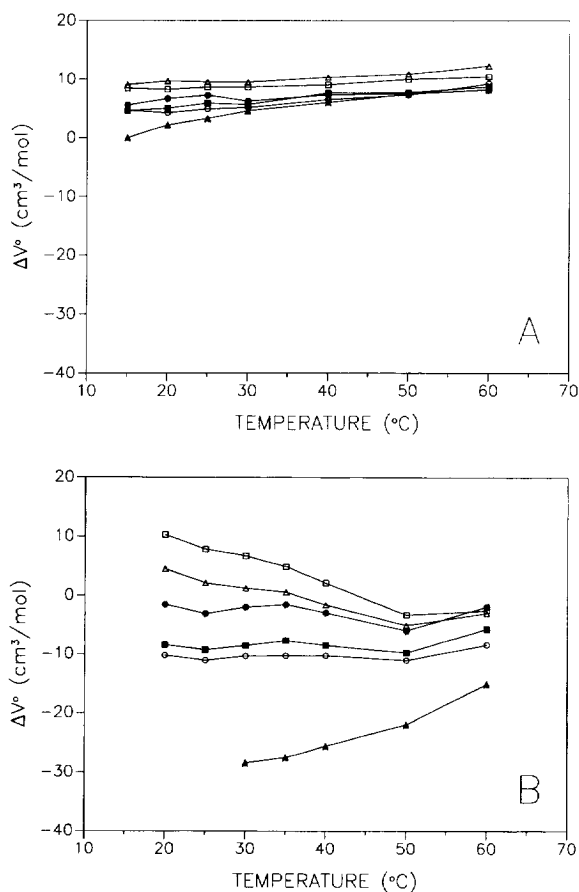


Fig. 6. Molar volume ( $\Delta V^\circ$ ) as a function of temperature for the benzene homologues. (A) monomeric octadecylsilica stationary phase with  $2.7 \mu\text{mol m}^{-2}$  bonding density, (B) polymeric octadecylsilica stationary phase with  $5.4 \mu\text{mol m}^{-2}$  bonding density. Solutes as given in Fig. 5; other experimental conditions as given in the text.

which represents the relative rate of change of molar volume to molar enthalpy, is greater for the methylene homologues than for the benzene homologues for both the low-density and high-density stationary phases.

Another distinction is that the methylene homologues exhibit a discontinuity in molar enthalpy and volume at the transition temperature of octadecylsilica, whereas the benzene homologues do not. The phase transition in octadecylsilica [3,5,29] and octadecanoic acid monolayers [30,31] is not a first-order transition (e.g., simple liquid–solid freezing or melting) but, rather, is a second-order transition that

occurs over a very wide temperature range. It is generally thought to be due to ordering or conversion of carbon–carbon bonds from the *gauche* to the *all-trans* form, beginning at the proximal or bound end of the chain and gradually progressing to the distal end [32]. This kind of phase transition is much more complex than a first-order transition, and will not affect all solutes in the same manner. The methylene homologues can penetrate deeply into the stationary phase [3–5] and, because of their template structure, are most greatly influenced by subtle changes in the octadecylsilica structure. In contrast, the benzene homologues may only be able to penetrate the distal region of the stationary phase. This premise is supported by the seminal study of Berendsen and De Galan [33], in which solute retention was measured as a function of the stationary phase chain length from 1 to 22 carbons. The benzene homologues, naphthalene and anthracene, exhibited a linear increase in retention up to a critical chain length of 10.9 and 12.2 carbons, respectively, with only a minor increase in retention thereafter. Thus, it seems unlikely that the benzene homologues are exposed to the proximal, more highly ordered regions of the stationary phase at the transition temperature. It has been noted that these homologues begin to exhibit smoothly varying changes in retention at lower temperatures [34–36], perhaps as the distal regions become more ordered.

#### 4. Conclusions

In this study, we report the first systematic measurements of the change in molar volume for methylene and benzene homologues. These measurements, when accompanied by the more traditional measurements of the change in molar enthalpy, can provide detailed information and insight concerning the equilibrium distribution of the homologous solutes between the mobile and stationary phases. Although the present study was limited to a simple chromatographic system with a pure methanol mobile phase and octadecylsilica stationary phases, it is apparent that this approach can now be applied with confidence to more complex systems. Such studies will be an essential step toward the evaluation and elucidation

Table 3  
Correlation of molar enthalpy ( $\Delta H^\circ$ ) and molar volume ( $\Delta V^\circ$ ) for the methylene homologues at 30°C

Solutes	Low-density octadecylsilica <sup>a</sup>		High-density octadecylsilica <sup>b</sup>	
	$\Delta H^\circ$ (kcal mol <sup>-1</sup> )	$\Delta V^\circ$ (cm <sup>3</sup> mol <sup>-1</sup> )	$\Delta H^\circ$ (kcal mol <sup>-1</sup> )	$\Delta V^\circ$ (cm <sup>3</sup> mol <sup>-1</sup> )
C <sub>10</sub>	-1.74	+1.92	-10.6	-27.1
C <sub>12</sub>	-2.19	+0.11	-14.2	-37.4
C <sub>14</sub>	-2.58	-0.68	-17.8	-51.7
C <sub>16</sub>	-2.97	-1.44	-21.4	-68.6
C <sub>18</sub>	-3.37	-2.33	-25.2	-83.4
C <sub>20</sub>	-3.79	-3.17	-28.1	-92.9
C <sub>22</sub>	-4.20	-4.31	-30.5	-104
Slope	2.37 cm <sup>3</sup> kcal <sup>-1</sup>		3.93 cm <sup>3</sup> kcal <sup>-1</sup>	
Intercept	5.64 cm <sup>3</sup> mol <sup>-1</sup>		16.6 cm <sup>3</sup> mol <sup>-1</sup>	
Correlation coefficient	0.987		0.997	

<sup>a</sup> Monomeric octadecylsilica stationary phase with 2.7  $\mu\text{mol m}^{-2}$  bonding density.

<sup>b</sup> Polymeric octadecylsilica stationary phase with 5.4  $\mu\text{mol m}^{-2}$  bonding density.

Table 4  
Correlation of molar enthalpy ( $\Delta H^\circ$ ) and molar volume ( $\Delta V^\circ$ ) for the benzene homologues at 30°C

Solutes	Low-density octadecylsilica <sup>a</sup>		High-density octadecylsilica <sup>b</sup>	
	$\Delta H^\circ$ (kcal mol <sup>-1</sup> )	$\Delta V^\circ$ (cm <sup>3</sup> mol <sup>-1</sup> )	$\Delta H^\circ$ (kcal mol <sup>-1</sup> )	$\Delta V^\circ$ (cm <sup>3</sup> mol <sup>-1</sup> )
Ph	-0.83	+6.27	-3.85	-2.01
Chr	-1.63	+5.69	-7.71	-8.57
Pic	-2.99	+4.62	-17.2	-28.4
Slope	0.77 cm <sup>3</sup> kcal <sup>-1</sup>		2.00 cm <sup>3</sup> kcal <sup>-1</sup>	
Intercept	6.92 cm <sup>3</sup> mol <sup>-1</sup>		6.16 cm <sup>3</sup> mol <sup>-1</sup>	
Correlation coefficient	1.000		0.998	

<sup>a</sup> Monomeric octadecylsilica stationary phase with 2.7  $\mu\text{mol m}^{-2}$  bonding density.

<sup>b</sup> Polymeric octadecylsilica stationary phase with 5.4  $\mu\text{mol m}^{-2}$  bonding density.

tion of the retention mechanism in reversed-phase liquid chromatography.

Chemical Sciences, under Grant Number DE-FG02-89ER14056.

## Acknowledgments

The authors are grateful to Dr. Lane C. Sander (National Institute of Standards and Technology) for performing the custom synthesis of the monomeric and polymeric octadecylsilica stationary phases, and to Dr. Stephen A. Wise (National Institute of Standards and Technology) for providing standard samples of the polynuclear aromatic hydrocarbons. This research was supported by the US Department of Energy, Office of Basic Energy Sciences, Division of

## References

- [1] R.J. Laub and R.L. Pecsok, *Physicochemical Applications of Gas Chromatography*, Wiley, New York, 1978.
- [2] J.R. Conder and C.L. Young, *Physicochemical Measurement by Gas Chromatography*, Wiley, New York, 1979.
- [3] A. Tchaplá, S. Heron, E. Lesellier and H. Colin, *J. Chromatogr. A*, 656 (1993) 81.
- [4] P.W. Carr, J. Li, A.J. Dallas, D.I. Eikens and L.C. Tan, *J. Chromatogr. A*, 656 (1993) 113.
- [5] J.F. Wheeler, T.L. Beck, S.J. Klatte, L.A. Cole and J.G. Dorsey, *J. Chromatogr. A*, 656 (1993) 317.

- [6] A. Vailaya and Cs. Horváth, *J. Phys. Chem.*, 100 (1996) 2447.
- [7] V.L. McGuffin and C.E. Evans, *J. Microcolumn Sep.*, 3 (1991) 513.
- [8] V.L. McGuffin, C.E. Evans and S.H. Chen, *J. Microcolumn Sep.*, 5 (1993) 3.
- [9] C.E. Evans and V.L. McGuffin, *Anal. Chem.*, 60 (1988) 573.
- [10] V.L. McGuffin and R.N. Zare, *Appl. Spectrosc.*, 39 (1985) 847.
- [11] L.C. Sander, National Institute of Standards and Technology, Gaithersburg, MD, personal communication (1993).
- [12] J.C. Gluckman, A. Hirose, V.L. McGuffin and M. Novotny, *Chromatographia*, 17 (1983) 303.
- [13] D.E. Martire, *J. Chromatogr.*, 461 (1989) 165.
- [14] S.H. Chen, Ph.D. Dissertation, Michigan State University, East Lansing, MI, 1993.
- [15] J.C. Sternberg, *Adv. Chromatogr.*, 2 (1966) 205.
- [16] D.W. Morton and C.L. Young, *J. Chromatogr. Sci.*, 33 (1995) 514.
- [17] V.L. McGuffin and S.H. Chen, *Anal. Chem.*, in press.
- [18] G. Guiochon and M.J. Sepaniak, *J. Chromatogr.*, 606 (1992) 248.
- [19] A. Tchaplá, H. Colin and G. Guiochon, *Anal. Chem.*, 56 (1984) 621.
- [20] L.C. Sander and S.A. Wise, *CRC Crit. Rev. Anal. Chem.*, 18 (1987) 298.
- [21] G.L. Gaines, *Insoluble Monolayers at Liquid–Gas Interfaces*, Wiley, New York, 1966.
- [22] N.K. Adam, *Physics and Chemistry of Surfaces*, Dover, New York, 1968, p. 64.
- [23] E.N. Washburn, *International Critical Tables of Numerical Data*, McGraw-Hill, New York, 1928, Vol. 3, p. 30.
- [24] I. Gutman and S.J. Cyvin, *Introduction to the Theory of Benzenoid Hydrocarbons*, Springer-Verlag, Berlin, 1989.
- [25] L.C. Sander and S.A. Wise, *Anal. Chem.*, 59 (1987) 2309.
- [26] S.A. Wise, W.J. Bonnett, F.R. Guenther and W.E. May, *J. Chromatogr. Sci.*, 19 (1981) 457.
- [27] C. Yan and D.E. Martire, *J. Phys. Chem.*, 96 (1992) 3505.
- [28] S.H. Chen and V.L. McGuffin, *J. Phys. Chem.*, in preparation.
- [29] J.C. Van Miltenburg and W.E. Hammers, *J. Chromatogr.*, 268 (1983) 147.
- [30] J.F. Baret, *Prog. Surf. Membr. Sci.*, 14 (1981) 291.
- [31] C.M. Knobler and R.C. Desai, *Ann. Rev. Phys. Chem.*, 43 (1992) 207.
- [32] A. Ulman, *An Introduction to Ultrathin Organic Films*, Academic Press, Boston, MA, 1991, pp. 133–141.
- [33] G.E. Berendsen and L. de Galan, *J. Chromatogr.*, 196 (1980) 21.
- [34] J. Chmielowiec and H. Sawatzky, *J. Chromatogr. Sci.*, 17 (1979) 245.
- [35] L.C. Sander and S.A. Wise, *Anal. Chem.*, 61 (1989) 1749.
- [36] K.B. Sentell and A.N. Henderson, *Anal. Chim. Acta*, 246 (1991) 139.